Bull. Mater. Sci. (2020) 43:1
https://doi.org/10.1007/s12034-019-1971-5

Some aspects of new Cu(NbC) films

CHON-HSIN LIN
General Education Center, Chung Yuan Christian University, Chung Li 320, Taiwan
f1213295152006@yahoo.com.tw

MS received 29 January 2019; accepted 20 June 2019

Abstract. In this study, new barrier-free Cu(NbC) alloy films with two different thicknesses, i.e., 8 and 300 nm, containing 0.3 at% C and 0.5 at% Nb, which are deposited *via* co-sputtering on three types of substrates, viz., Si, stainless steel and polyimide (PI), have been developed, annealed, measured and analysed. The resistivity value of the new 300-nm-thick films atop Si substrates is 3.07 $\mu\Omega$ cm after annealing at 450°C for 200 h. The low resistivity and diffusion depth of the new films exhibit their good quality in anti-oxidation stability in a high-temperature environment. The films also display high-adhesive strength atop either stainless-steel or PI substrates, ~7–8 times greater than that of their pure-Cu counterparts. In sharp contrast, the antibacterial ratio of the new films is ~96% while that of their pure-Cu counterparts is 0%. In addition, the contact angles of Cu(NbC) films are greater than those of their pure-Cu counterparts, resulting in a far superior antibacterial efficacy for the new films to pure-Cu films against, for example, *Staphylococcus aureus* BCRC 10451. With these desirable merits, the new films seem to be a good candidate material for bacteria killing and prevention, reduction of legionella spread inside hospitals and/or large buildings, biological medical care systems and advanced surgical tools. The new films deposited on PI substrates also seem to be suitable for making supple electrically conductive parts or devices, such as flexible panels, keyboards, screens, smartphones embedded in smart textiles and so forth.

Keywords. Cu(NbC) alloy; films; co-sputtering; anti-oxidation; adhesive strength; bacteria killing and prevention.

1. Introduction

The medical application of copper (Cu) can be traced back to 2600 BC when Egyptians adopted it to cure chest wounds and kill bacteria in drinking water [1]. The once-known bacteria-killing/prevention method using copper gradually diminished after development of antibacterial drugs in 1932 [2]. However, owing to the widespread existence of antibiotic-resistant bacteria in medical environments nowadays, clusters of antibiotic-resistant bacteria in healthcare institutions could outburst when inadequate contamination–prevention measures occur [2]. The development of antibiotics capable of resisting new bacterial transformation has been slower than what is expected or needed. How to prevent the spreading of multidrug-resistant bacteria in medical care units has become a primary contamination control subject in many hospitals [3]. The antibacterial application of Cu has, therefore, re-gained greater attention, and further studies are needed to make the medical application possesses wider and more durable effects [4]. Many objects having daily contact with humans and/or patients in medical environments and/or inside large buildings open to public, such as door handles, handrails, bed-guard rails, call bells, faucets, etc., are made of stainless steel with merits such as ease of cleaning and anti-corrosion [5]. Stainless steel, however, does not help in fighting off bacteria, and it is often contaminated by various types of bacteria [6]. Hence, if we can replace stainless steel with copper or have the stainless steel coated with a copper or proper copper alloy surface, we will resolve bacteria spreading more effectively, the reason for which is given below.

Copper usually can deactivate bacteria within hours [7]. The mechanism of bacteria-killing through copper contact lies in the fact that copper ions cause cell death by destroying cell membranes, producing oxygen radicals and destroying cell DNA [8]. The higher the copper substance in an alloy, the greater will be the alloy's bacteria-killing efficacy. However, once copper oxide (CuO) is formed on a copper surface, the antibacterial efficacy of copper will be weakened [7]. Mikolay *et al* [7] found that the bacteria count is the least on a copper surface, followed by an aluminium surface and, next, a stainless-steel surface. In 1994, Liu *et al* [9] verified that copper–silver ionization can effectively reduce the positive rate of legionella inside the water supply pipes of medical-care institutes so as to reduce legionella spread inside hospitals, arousing new attention to using of copper to suppress bacteria.

As Cu is widely used in various metallization processes [10,11], we have encountered that under high temperatures, Cu is prone to diffuse into Si or SiO_2, resulting in the formation of Cu_3Si, a silicide which undesirably increases Cu-film resistivity. To avert the diffusion, inserting a barrier between Cu and Si, was proposed and has been tried [12–14]. However, when the thickness of the barrier layer reduces to a nanometre range, some detrimental events, such as electron and grain

Published online: 27 November 2019

boundary scattering, may take place, resulting in an increase in resistivity [15] in microelectronic components produced with this method. According to our previous studies [16–18], we have found that by co-sputtering, materials immiscible with Cu to form Cu-alloy films between Cu and Si, we can render with two advantages for the metallized products that use the films, i.e., high-thermal anti-oxidation stability and low resistivity. The main reason for mixing immiscible Nb and C into Cu in the study is due to their high-melting points, 2477 and 3675°C, respectively, which help avert Cu oxidation and hence maintain the antibacterial efficacy of the Cu alloy. The films were fabricated *via* co-sputtering and then annealed, measured and analysed in various aspects, such as electric resistivity, adhesive strength, antibacterial efficacy against *Staphylococcus aureus* BCRC 10451, antibacterial ratio and so on, so as to reveal their key characteristics for medical and/or industrial use. Stainless-steel substrates are used to emulate the regular hospital/medical care environments and/or large buildings open to public where stainless steel is widely used while PI substrates are used to exploit the merits of PI, including its (a) tolerance/resistance on both high and low temperatures and corrosion from chemical liquids and gases, (b) low heat-related expansion and high dimensional stability, (c) high flexural strength and so on.

The Cu(NbC) films developed in this study seem to be a good candidate material in medical use, particularly for bacteria killing and prevention, reduction of legionella spread inside hospitals, biological medical care, surgical tools, etc. Although silver (Ag) is also effective in bacteria-killing, its effect-continuity, however, is limited for its efficacy as bacteria-killing deteriorates with the contact of light and chlorine, both of which are unavoidable in a human-living environment, not to mention its cost which is far more expensive than copper (silver spot price is $15.45/Lb and copper $2.6/Lb, as of 2 January 2019 as displayed on Stock Market Watch, a website in the USA) [19].

The new films deposited on PI substrates also seem to be suitable for making supple electrically conductive parts or devices, such as flexible panels, keyboards, screens, smartphones embedded in smart textiles and so on. This study joins a new study field in materials science in meeting progressive medical and industrial needs. The main contribution of the study is the introduction of new Cu(NbC) films for the field, and their key features and possible applicable usage are herein described.

2. Experimental

To fabricate the films, we first co-sputtered Cu, Nb and C atop Si, stainless-steel or PI substrates under an Ar atmosphere of 10^{-4} Torr to form new Cu(NbC) films with two different thicknesses, 8 and 300 nm. The new films contain 0.3 at% C and 0.5 at% Nb, as measured by an electron probe microanalyser (EPMA) adopted in the study. Other compositions explored during the search for an optimal or nearly optimal composition structure in the study include 0.5 and 0.2 at% C together with 0.4 and 0.7 at% Nb, which are all measured using the EPMA. We then placed the films within a vacuum at 10^{-7} Torr and heated them up to isothermally anneal them at 200, 400, 530 and 750°C for 1 h, or cyclically anneal them. The objective of cyclic annealing is to examine if the films are prone to oxidation in rapidly temperature-changing environments. The cyclic annealing processes are carried out in the following steps: first, the vacuum pressure was set at 10^{-7} Torr, and its temperature was increased from room temperature to 400–600°C and then instantly stopped and cooled back to room temperature, which comprises a cycle. Next, five said cycles were repeatedly implemented without a holding temperature. The heating and cooling rates during each cycle were 6.7 and 10°C min^{-1}, respectively.

The adhesion property of the films was evaluated by measuring their pull-off strength according to ASTM International standard D4541-02.27 [20]. The crystal structures and microstructures of the films before and after annealing were measured and analysed using X-ray diffraction (XRD), focused ion-beam microscopy, transmission electron microscopy (TEM) and X-ray energy dispersive spectroscopy. In addition, the film resistivity values were measured at room temperature using the four-point probe method.

Antibacterial tests on the new films were performed using the method outlined in JIS Z 2801 [21], a Japanese industry standard for evaluating anti-microbial efficacy in antimicrobial products. The results show that the annealed films exhibit low resistivity, low-leakage current and strong adhesion to their substrates. No silicides or oxides were formed during vacuum annealing. With an antibacterial ratio being calculated as follows:

$$\text{Antibacterial ratio } (R)\% = [(A - C)/A] \times 100$$

where A denotes the total bacteria count on a pure-Cu film cumulated after 24 h and C is the same as A but for a Cu-alloy film instead, the antibacterial studies using *Staphylococcus aureus* BCRC 10451 were executed and completed.

3. Results and discussion

The XRD patterns of both the new Cu(NbC) alloy films and pure-Cu films are shown in figure 1 for comparison. Figure 1a and b shows the XRD pattern of Cu(NbC) films as-deposited and after annealing at 600°C for 1 h, in which we observe that there exists an NbC phase (JCPDS 5-0658) dissolved as a solid solution within pure Cu, and owing to the minute amount of NbC, its peaks are relatively weak. We also observe that for Cu peaks no phase shift appears and that there appear no compounds formed by the reactions between Cu and Nb or between Cu and C. Figure 1b reveals that Nb and C are

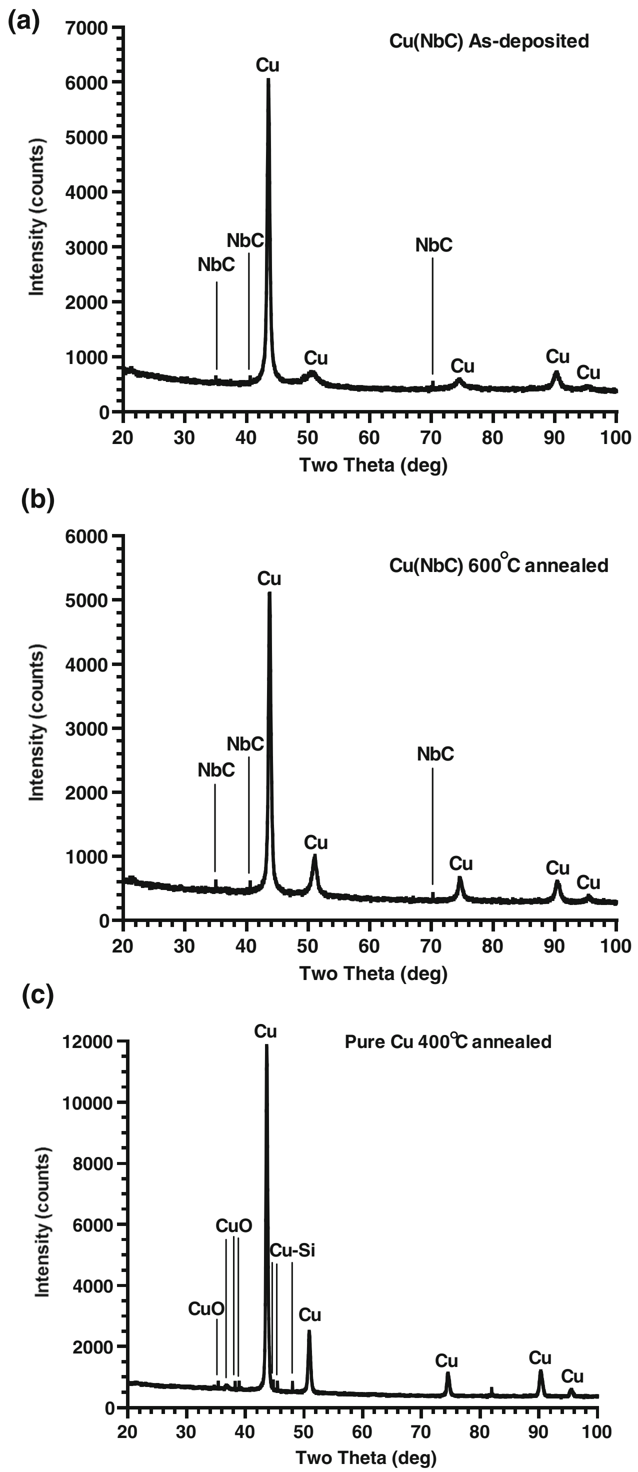

Figure 1. (**a**) XRD pattern of the Cu(NbC) alloy films as-deposited, (**b**) the XRD pattern of the films after annealing at 600°C for 1 h and (**c**) for comparison, the XRD pattern of pure-Cu films after annealing at 400°C for 1 h [18].

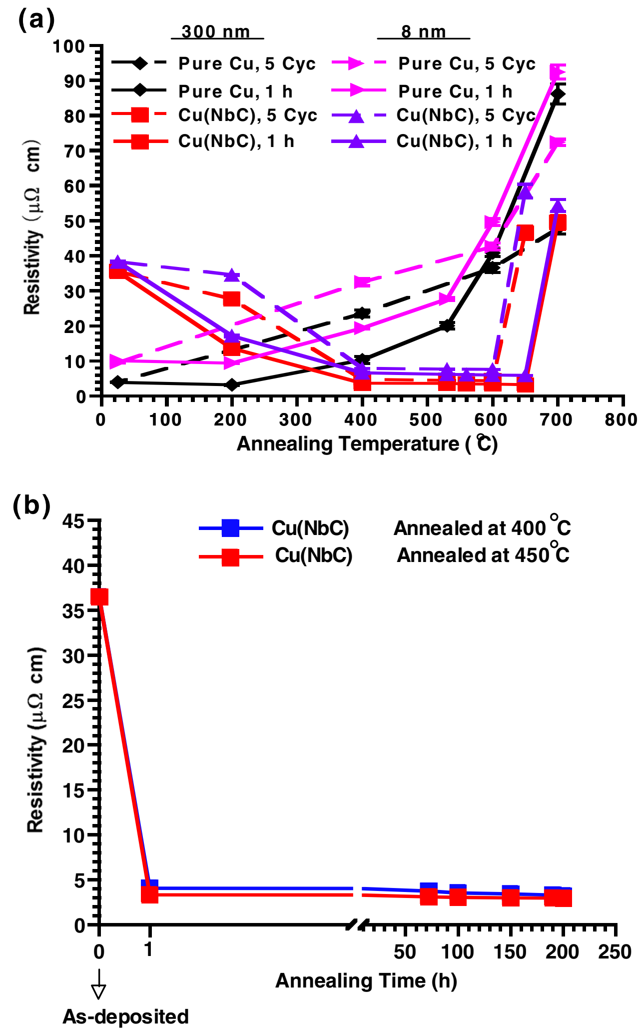

Figure 2. (**a**) Resistivity curves of Cu(NbC) and pure-Cu films, with thicknesses of 8 or 300 nm and sputtered on barrier-free Si substrates, after isothermal and cyclic annealing at various temperatures for various durations as listed inside the figure and (**b**) the resistivity curves of 300-nm-thick Cu(NbC) films after annealing at 400 or 450°C for 200 h.

still dissolved in the film as solid solution, verifying the high-thermal stability of the alloy film. Figure 1c shows that CuO and Cu–Si compounds emerged after pure-Cu films had been annealed at 400°C for 1 h. The comparison verifies that when the NbC phase emerges in a Cu-alloy film as solid solution, the NbC phase can boost the thermal stability of the film up to 600°C.

The resistivity of the Cu(NbC) films after we increased or decreased their Nb and C amounts and annealed them isothermally at 400°C for 1 h, or treated them with cyclic annealing processes, lies in a range of 3.62–8.45 μΩ cm. The resistivity reaches its lowest value when the composition structure of the films is set at 0.3 at% Nb and 0.5 at% C, which is the only composition structure thus adopted throughout the present study. The resistivity measurement results for 8- and 300-nm-thick Cu(NbC) films as deposited on barrier-free Si substrates are shown in figure 2a. The as-deposited film resistivity appears higher (∼35.46 μΩ cm) in figure 2a owing to the formation of the NbC phase. The resistivity substantially decreases during annealing owing to stress relief, grain growth and a decrease in the defect concentration. After annealing at 400°C, the resistivity of Cu(NbC) films continuously decreases as annealing temperature increases. The resistivity of the films undergoing isothermal and cyclic annealing at 650 and 600°C lies at ∼3.21−4.35 μΩ cm. An abrupt resistivity increase as shown in figure 2a, however, is incurred owing to the formation of Cu_3Si. When Cu(NbC) films treated with isothermal and cyclic annealing reach their maximal thermal stability corresponding to 650 and 600°C, respectively, and their resistivity values are 3.21 and 4.35 μΩ cm, respectively. As the film thickness reduces to 8 nm, the film resistivity increases. Such an increase is most apparent in a pure-Cu film but less apparent in a Cu(NbC) film. Figure 2b shows the resistivity variations of Cu(NbC) films after they were separately annealed at 400 and 450°C for 200 h. The two separate films exhibit a continuous resistivity decrease during annealing, and low resistivity indicates that no reactions occurred between Cu and Si during annealing. A sustaining stable resistivity is an important index for film reliability. The thinner the film, the higher the resistivity, and this is caused by grain boundary scattering owing to smaller-sized grains [22,23]. The resistivity values of 300-nm-thick Cu(NbC) films after annealing separately at 400 and 450°C for 200 h are 3.14 and 3.07 μΩ cm, respectively. This indicates that the NbC dissolved as solid solution in the films has suppressed film oxidation.

Figure 3a and b shows the cross-sectional TEM images of a pure-Cu film after annealing at 400°C for 1 h. From figure 3b, we observe that CuO and Cu–Si compounds are

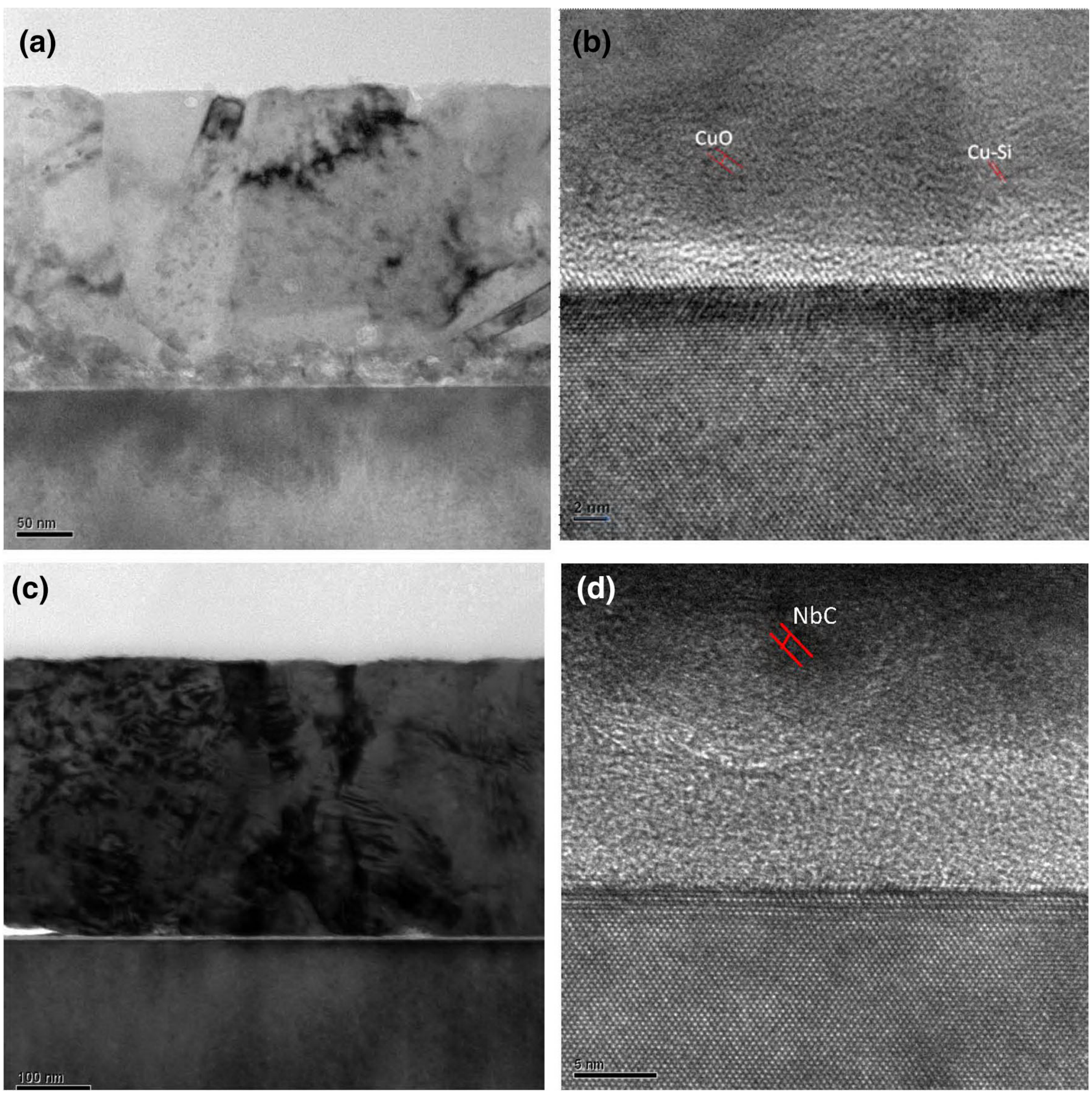

Figure 3. Pure Cu (**a**) TEM and (**b**) high-resolution TEM images after annealing at 400°C for 1 h; Cu(NbC) alloy (**c**) TEM and (**d**) high-resolution TEM images after annealing at 650°C for 1 h (film thickness: 300 nm).

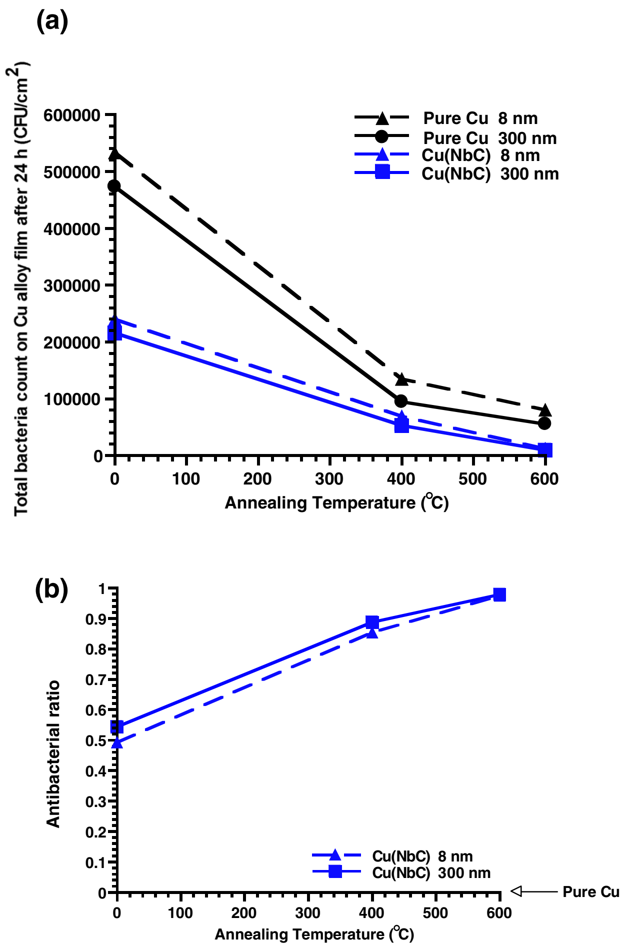

Figure 4. Antibacterial efficacy against *S. aureus* BCRC 10451 of the Cu(NbC) alloy and pure-Cu films, of various thicknesses and prior to and after annealing, after 24 h of bacteria exposure—in comparison with that of pure-Cu films, i.e., (**a**) bacteria count and (**b**) antibacterial ratio.

formed owing to oxidation, which is in line with the XRD result of the pure-Cu film shown in figure 1c. Figure 3c and d shows the cross-sectional TEM images of a Cu(NbC) film after annealing at 650°C for 1 h. From figure 3d, we observe a 2.56 Å d-spacing NbC phase dissolved in the film as solid solution, which increases the thermal stability of the film owing to the suppression of the phase upon oxidation and the reaction between Cu and Si. The diffusion depth of the new film is lower than that of the pure-Cu film. The result is in line with the XRD result of the new film shown in figure 1b.

Figure 4 shows the bacteria count and antibacterial ratio of *S. aureus* BCRC 10451 on 8- and 300-nm-thick Cu(NbC) alloy films and pure-Cu films after 24 h of bacteria exposure, wherein figure 4a indicates the bacteria count and figure 4b indicates the antibacterial ratio. From figure 4a and b, we observe that in comparison with pure-Cu films, the antibacterial efficacy of Cu(NbC) alloy films is far superior to their

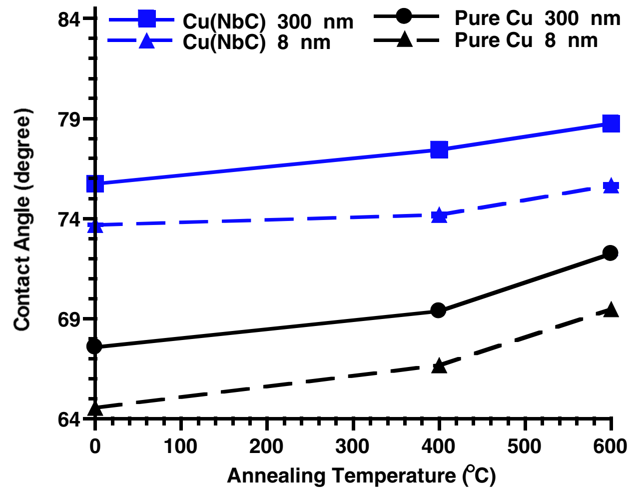

Figure 5. Contact-angle variations of Cu(NbC) films in comparison with that of pure-Cu films, before and after annealing.

pure-Cu counterparts. The antibacterial ratio of the 8- and 300-nm-thick Cu(NbC) alloy films is ∼96% after annealing at 600°C for 1 h while that of pure-Cu films is zero (0), a great contrast indeed. The antibacterial ratio varies from ∼49 to 96% for an 8-nm-thick alloy film and ∼54 to 96% for a 300-nm-thick alloy film when annealed from 0 up to 600°C. This ratio range is higher or far higher than that of the same films as-deposited, i.e., ∼49 and 54% for the 8- and 300-nm-thick Cu(NbC) films, respectively.

The contact angles of liquid drops on the new alloy Cu(NbC) films are noticeably greater than those of pure-Cu films, as shown in figure 5. The contact-angle variation of two types of films with a thickness of 8 and 300 nm before and after annealing is exhibited in figure 5. The physics behind the contact-angle variation is explained as follows. Cohesion or a cohesive force is linked to the intra-force among the same kinds of molecules while adhesion or an adhesive force is linked to the inter-force among different kinds of molecules. When cohesion is greater than adhesion, the contact angle, θ, of a liquid drop on and with respect to a horizontal solid–substrate surface plane, as shown in figure 6, becomes a dull angle; when cohesion is smaller than adhesion, θ becomes a sharp angle. Impurities added to a pure-metal substrate will alter its surface tension with the following results:

(1) Cohesion > adhesion, if the molecules within the substrate are (substantially) non-hydrogen-bound (non-H-bound);
(2) Cohesion < adhesion, if the molecules within the substrate are (substantially) H-bound.

Accordingly, the NbC phase representing impurities and non-H-bound molecules dissolved as solid solution in the crystal lattices of pure Cu and converting the pure Cu into Cu(NbC) in the present study shall make the cohesive force

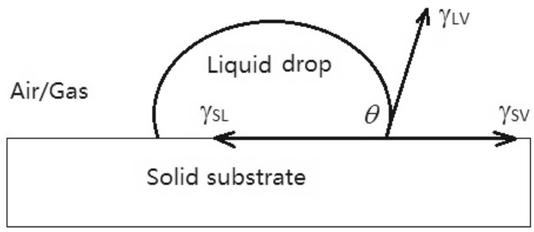

Figure 6. Anatomy of the contact angle.

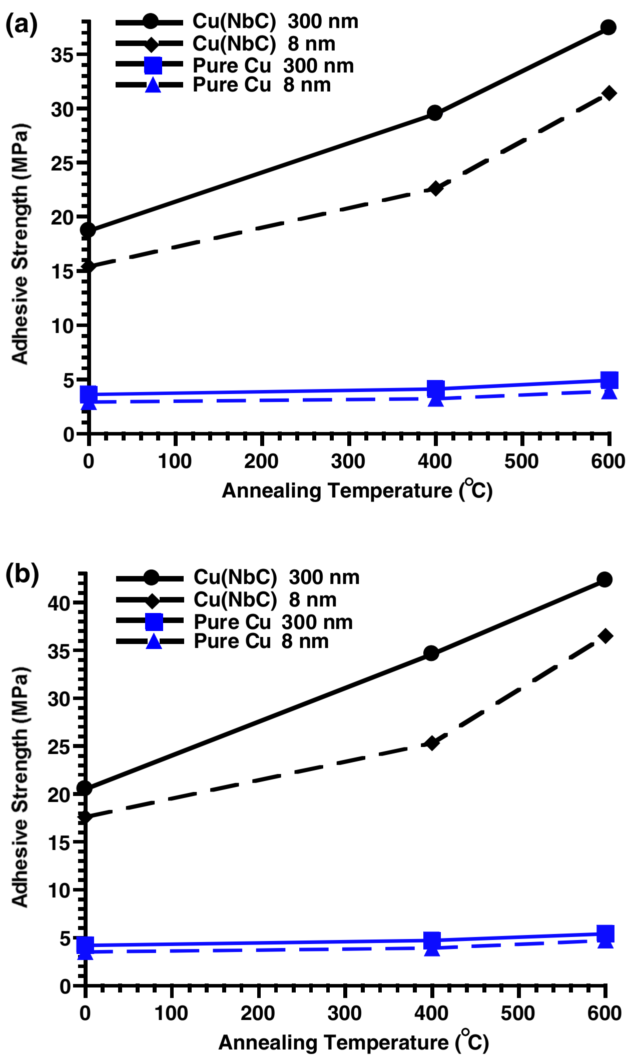

Figure 7. Adhesion test results of pure-Cu and Cu(NbC) films as-deposited and after annealing at 600°C for 1 h for two different film-thicknesses of (**a**) 8 and (**b**) 300 nm.

greater against a liquid drop on the Cu(NbC) substrate surface, causing the contact angle on a Cu(NbC) substrate greater than that of its pure-Cu counterparts. This is verified in the test results as exhibited in figure 5. In addition, annealing the new films can further increase their contact angles as shown in figure 5. The contact angles of the as-deposited films are smaller since the grain sizes within the films are smaller prior to annealing, i.e., 22 ± 3 nm, causing the films looser and less dense. After annealing, the grain sizes grow up to 45 ± 3 nm, causing the films more compact and denser and having greater contact angles. Since smaller contact angles on the films will make the films gluier to bacteria and greater contact angles will make the films less gluey to bacteria, the Cu(NbC) films offering greater contact angles thus render greater antibacterial efficacy than their pure-Cu counterparts.

Figure 7 shows the ASTM D4541-02 adhesion test results of both 8- and 300-nm-thick pure Cu and Cu(NbC) films, as-deposited on either stainless-steel or PI substrates, all barrier-free or after being annealed at 600°C for 1 h. The adhesion strength of the 300-nm-thick, as-deposited Cu(NbC) alloy films, i.e., 18.7 ± 0.1 MPa, is 5–6 times that of pure-Cu films, both on stainless-steel substrates, and grows to 20.5 ± 0.2 MPa, or 4–5 times that of pure-Cu films, both on PI substrates. The adhesion strength of the same Cu(NbC) films after annealing at 600°C for 1 h increases to 37.4 ± 0.2 MPa (figure 7a), which is 7–8 times that of pure-Cu films, both on stainless-steel substrates, and to 42.3 ± 0.1 MPa (figure 7b), which is 7–8 times that of pure-Cu films, both on PI substrates. When the film thickness is reduced to 8 nm, adhesion strength of the Cu(NbC) film remains at a comparably high level, a phenomenon similar to that of Cu(RuN_x) films [24]. This might be due to the NbC segregated at the film interface, which is an intuition that still needs to be verified in future studies.

4. Conclusion

In this study, new barrierless Cu(NbC) alloy films being 8 and 300 nm in thickness and containing 0.3 at% C and 0.5 at% Nb were deposited *via* co-sputtering on Si, stainless-steel or PI substrates, and then sequentially annealed, measured and analysed. The resistivity of the new 300-nm-thick films reduces to 3.14 and 3.07 μΩ cm after they were annealed at 400 and 450°C, respectively, for 200 h, verifying the high-thermal anti-oxidation stability of the new films. The diffusion depth of the films is also lower than that of pure-Cu films.

The low resistivity and diffusion depth of the new films indicate a feature of high-thermal anti-oxidation stability. The 300-nm-thick films deposited on stainless-steel substrates, which emulate their possible application to stainless-steel-made products widely used in medical environments and/or large buildings open to public, display high-adhesive strength, ∼7–8 times higher than that of pure-Cu films. The antibacterial ratio against, e.g., *S. aureus* BCRC 10451 of the 8- and 300-nm-thick new films, ∼96%, is far better than the zero antibacterial ratio of their pure-Cu counterparts. In addition, the contact angles rendered by Cu(NbC) films are greater than that of pure-Cu films, and, hence, the antibacterial efficacy of the new films is substantially superior to that of pure-Cu films.

With the mentioned merits, the new alloy films seem to be a good candidate material for bacteria killing and prevention, reduction of legionella spread inside hospitals or large buildings, biological medical care systems and advanced surgical tools. The new films with PI substrates can also be applied to supple electrically conductive parts and components, future smartphones embedded in smart textiles and so forth. The main contribution of the study is the introduction of new Cu(NbC) films for the materials science field and their key features and applicable medical and industrial usage are explored herein.

Acknowledgements

This work was sponsored by the National Science Council of the Republic of China in Taiwan, under Project No. MOST 105-2221-E-243-001.

References

[1] Grass G, Rensing C and Solioz M 2011 *Appl. Environ. Microbiol.* **77** 1541
[2] Santo C E, Quaranta D and Grass G 2012 *Microbiologyopen* **1** 46
[3] Rensing C and Grass G 2003 *FEMS Microbiol. Rev.* **27** 197
[4] Franke S, Grass G, Rensing C and Nies D H 2003 *J. Bacteriol.* **185** 3804
[5] Dupont C L, Grass G and Rensing C 2011 *Metallomics* **3** 1109
[6] Singh Satish K, Grass G, Rensing C and Montfort William R 2004 *J. Bacteriol.* **186** 7815
[7] Mikolay A, Huggett S, Tikana L, Grass G, Braun J and Nies Dietrich H 2010 *Appl. Microbiol. Biotechnol.* **87** 1875
[8] Santo C E, Lam E W, Elowsky Christian G, Quaranta D, Domaille Dylan W, Chang Christopher J *et al* 2011 *Appl. Environ. Microbiol.* **77** 794
[9] Liu Z, Stout J E, Tedesco L, Boldin M, Hwang C, Diven W F *et al* 1994 *J. Infect. Dis.* **169** 919
[10] Kang S K, Shih D Y, Fogel K, Lauro P, Yim M J, Advocate G G *et al* 2002 *IEEE Trans. Electron. Packag. Manuf.* **25** 155
[11] Ho C E, Yang S C and Kao C R 2007 *J. Mater. Sci.: Mater. Electron.* **18** 155
[12] Wang Y, Tang B-H and Li F-Y 2016 *Vacuum* **126** 51
[13] Fei C, Wu G-H, Jiang L-T and Chen G-Q 2015 *Vacuum* **122** 122
[14] Wang Y, Chen X, Ma W, Shang Y, Lei Z and Xiang F 2017 *Appl. Surf. Sci.* **396** 333
[15] Lozano J G, Lozano-Perez S, Bogan J, Wang Y C, Brennan B, Nellist P D *et al* 2011 *Appl. Phys. Lett.* **98** 123112
[16] Lin C-H 2015 *Jpn. J. Appl. Phys.* **54** 05ED04
[17] Lin C-H 2017 *Jpn. J. Appl. Phys.* **56** 01AB09
[18] Lin C-H 2016 *Jpn. J. Appl. Phys.* **55** 06JD02
[19] http://thestockmarketwatch.com/metal/prices.aspx
[20] ASTM D4541-02 2002 Vol. 06.1
[21] Jis Z 2801 Test method
[22] Rossnage S M and Kuan T S 2004 *J. Vac. Sci. Technol. B* **22** 240
[23] Barmak K, Cabral C Jr, Rodbell K P and Harper J M E 2006 *J. Vac. Sci. Technol. B* **24** 2485
[24] Chu J P, Lin C H and John V S 2007 *Appl. Phys. Lett.* **91** 132109